Journal of
Materials Chemistry A

Materials for energy and sustainability

Accepted Manuscript

This article can be cited before page numbers have been issued, to do this please use: H. Huang, Y. Zhou, Y. Wang, X. Cao, C. Han, G. Liu, Z. Xu, C. Zhan, H. Hu, Y. Peng, P. Yan and D. Cao, *J. Mater. Chem. A*, 2020, DOI: 10.1039/D0TA06191C.

This is an Accepted Manuscript, which has been through the Royal Society of Chemistry peer review process and has been accepted for publication.

Accepted Manuscripts are published online shortly after acceptance, before technical editing, formatting and proof reading. Using this free service, authors can make their results available to the community, in citable form, before we publish the edited article. We will replace this Accepted Manuscript with the edited and formatted Advance Article as soon as it is available.

You can find more information about Accepted Manuscripts in the Information for Authors.

Please note that technical editing may introduce minor changes to the text and/or graphics, which may alter content. The journal's standard Terms & Conditions and the Ethical guidelines still apply. In no event shall the Royal Society of Chemistry be held responsible for any errors or omissions in this Accepted Manuscript or any consequences arising from the use of any information it contains.

ROYAL SOCIETY OF CHEMISTRY

rsc.li/materials-a

View Article Online
DOI: 10.1039/D0TA06191C

Precise Molecular Design for B-N Modified Polycyclic Aromatic Hydrocarbon Toward Mechanochromic Material

Received 00th January 20xx,
Accepted 00th January 20xx

DOI: 10.1039/x0xx00000x

Huanan Huang*[a], Ying Zhou[a], Yawei Wang[a], Xiaohua Cao[a], Chuan Han[a], Guochang Liu[a], Zhixiong Xu[a], Changchao Zhan[a], Huanan Hu[a], You Peng[a], Ping Yan[a], Dapeng Cao*[b]

The development of intelligent materials, in particular those exhibiting the highly sensitive mechanochromic luminescent (MCL), is desirable but challenging since the MCL internal mechanism and the structure-performance relationship still remain unclear. Here, we report a new MCL material (BN benzo[f]tetraphene) using a molecular-level design strategy by introducing BN unit to a π-conjugated system. By investigating the BN benzo[f]tetraphene (**5**) and its analogue, it is found that the introduction of boron-nitrogen unit is the key to tailoring the molecular dipole moment and intermolecular interactions, which can therefore form the easily deformable molecular stacking pattern and endow **5** with wonderful MCL properties. The theoretical calculations confirm that the inherent energies like the excited singlet (S) and highly sensitive triplet (T) states exist in the MCL process, and the formation and fracture of ordered molecular aggregates have a significant effect on radiative and nonradiative transitions. The material also shows the high-contrasted and self-reversible properties related to the thermal-and force-stimulus, which makes it a promising candidate for security ink, optical recording applications. This work possibly opens up a new way to develop the efficient organic smart materials and therefore trigger the discovery of new functions and properties of azaborine compounds.

Introduction

The creative design and precise synthesis of novel mechanochromic luminescent (MCL) materials have attracted a great deal attention for their promising potential applications in security systems, memory devices, health monitoring, and so forth. [1-8] Since the pioneering work reported by Francis Bacon in 1605, [9-11] the MCL chemistry has been well established by numerous groups. Their endeavors have greatly impelled various building blocks being used as the core units to construct MCL luminogens, including tetraphenylethylene, phenothiazine and carbazole.[12-22] However, so far, due to lack of reliable guidance and unclear intrinsic mechanism,[23-26] how to control the MCL behaviors through the rational molecular design is still an enormous challenge. Therefore, the development of universal molecular design principle is crucial to break through this bottleneck, which not only provides the possibility to incessantly explore the potential performance of these materials in device applications, but also renders the opportunity to systematically investigate the inherent mechanism and their structure-MCL-property relationships. It is of great importance both in the fundamental research and practical applications in the future.

Actually, several strategies concerning the molecular design have been proposed to promote the mechanical stimulation responsive performances.[27-34] The appropriate crystallization capability with deformable packing patterns in principle is essential for excellent MCL,[35] which facilitate their phase transformation in the solid state. Stated differently, a rigid backbone should be involved in designing target molecule to maintain its molecular structure during the compressing process, as well as a relatively deformable packing mode to provide enough flexible space for molecular rearrangements. Particularly, the intermolecular interactions and molecular packing modes are the two key factors in modifying the molecular luminescence properties, [36-37] offering vital detail for understanding photophysical processes of different emissive forms. Rational balance of different intermolecular interactions and effective adjustment of the packing modes are thus tackled as crucial issues in the design of current mechano-responsive luminescent materials. The incorporation of main-group elements into polycyclic aromatic hydrocarbons (PAHs) is a promising strategy for modulation of the intermolecular interactions.[38-46] Among various possible dopants, boron and nitrogen-containing conjugated materials have been targeted for particular focus due to their distinct electronic and optical characteristics.[47-53] The replacement of C=C fragments with isoelectronic B-N units has been proved to be a powerful approach to tailor molecular packing modes and photophysical properties.[54-63] However, this strategy with applied potential in exploring the mechanoresponsive behaviors of BN-modified luminescent materials has long been neglected. Thus, it is fascinating to probe and verify the MCL characteristics of B-N/C=C isosterism at the molecule level.

Considered all the above points, herein, we synthesize the parental BN-embedded benzo[f]tetraphene **5** as a novel building block to discuss its possible MCL effect using precise molecular design strategy (Figure 1A).The molecule skeleton **5** contains a proper conjugate size, ensuring that the molecule presents crystalline state, which is an essential condition to explore the macroscopic performance of organic materials in the aggregates. Meanwhile, the planar conjugated fused ring, as an issue of interest in highly efficient emission, is the prerequisite for excellent MCL materials. More importantly, the insertion of boron nitrogen unit may prompt special molecular packing patterns to form in aggregated states, enhancing the possibility of MCL behavior. To highlight the importance of BN-incorporation into PAHs, its hydrocarbon analogue **5′** is served as a counterpart for comparison. Results indicate that the more polarized nature of the B-N bond in **5** than C=C bond in **5′** significantly alters the polarity of **5** and intermolecular forces, which favors the adjustment of arrangement and interactions

[a] School of Chemistry and Environmental Engineering; Jiangxi Province Engineering Research Center of Ecological Chemical Industry; Jiujiang Key Laboratory of Organosilicon Chemistry and Application, Jiujiang University, Jiujiang 332005, China. E-mail: huanan200890@163.com
[b] State Key Laboratory of Organic-Inorganic Composites, Beijing University of Chemical Technology, Beijing, 100029, China. E-mail: caodp@mail.buct.edu.cn

View Article Online
DOI: 10.1039/D0TA06191C

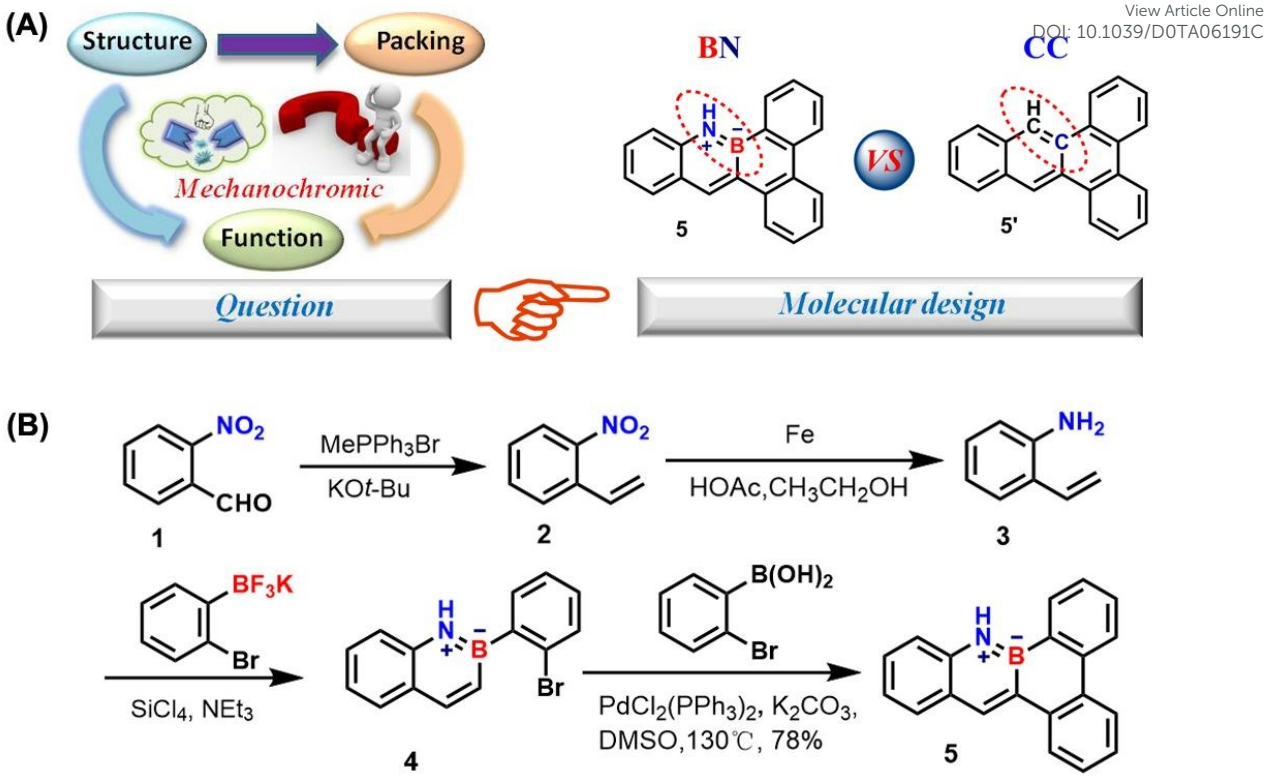

Figure 1. (A) The design strategy and target molecule for MCL materials; **(B)** Synthetic route to BN-benzotetraphene

of the molecule toward force-responsive characteristics. Compared to **5′**, the boron atom-induced the exposure of N-H bond in **5** can enhance the intermolecular interactions through possible N-H···π interactions, which is also a favorable factor for regulating molecular stacking pattern. In addition, the internal mechanism and potential application of **5** as the MCL smart materials are also investigated. These meaningful findings provide a new platform to construct BN-based MCL materials, which open a new window for the development of intelligent luminescent materials.

Results and discussion

The synthetic route of BN benzo[f]tetraphene was illustrated in Figure 1B. Commercially available 2-nitrobenzaldehyde **1** was initially converted to **2** through a witting reaction in 80% yield. Followed by iron powder used to reduce the nitro-group, compound **3** in 50% yield was generated. Afterwards, substrate **3** was efficiently cyclized with 2-bromophenyl trifluoroborane potassium salt under slightly modified conditions from the procedure reported by Molander,[64] yielding BN-naphthalene derivative **4** in 75%. The BN-naphthalene **4** is an ideal substrate for the tandem reactions since it features an active C–Br bond, which allowed us to perform further reactions to extend the π conjugation for improved molecular properties through palladium-catalyzed cross-coupling reactions. Subsequently, the key tandem reactions of **4** with 2-bromophenyl boronic acid were performed. Excitingly, the bromophenyl-substituted BN-naphthalene **4** was easily converted into the stable BN-benzo[f]tetraphene **5** in good yield. The crude products were stable enough for purification by column chromatography on silica gel. The structure of **5** was characterized systematically by ^{1}H, ^{13}C and ^{11}B NMR spectroscopy, high-resolution mass spectrometry and well corresponded with its expected structure.

The compound **5** exhibited superior stability under ambient conditions. Even in the destructive tests, no change of the absorption features was observed after stirring in dilute acidic and basic aqueous solutions. Thermogravimetric analysis in Figure S1 indicate that only 5% weight loss of **5** appears ataround 330 ℃, manifesting its high thermal stability. Such remarkable thermal stability is crucial for their applications in materials science.

To examine detailed photophysical properties of the BN-embedded molecule **5**, UV-vis absorption and fluorescence emission spectroscopies were carried out. The solvatochromic effects of **5** in various polar solvents were investigated as well given that the compound **5** may possess the charge transfer (CT) characteristics due to the polar B-N bond. The absorption and emission properties of **5** in CH_2Cl_2, n-hexane and toluene exhibit relatively weak solvatochromism (Figure S2-S3). The results indicated that the CT interactions in this compound was ignorable, which may be a result of the delocalized BN double-bond characteristics in this system. To explain this phenomenon, density functional theory (DFT) calculations were further performed at the B3LYP/6-31G(d) level to explore the electronic distribution of molecule **5**. As shown in Figure S4 in Supporting Information, both HOMO and LUMO orbitals delocalized over the whole aromatic skeleton, unlike the typical CT system exhibiting completely separated HOMO and LUMO levels,[65-66] only slight charge separation can be found in **5**

View Article Online
DOI: 10.1039/D0TA06191C

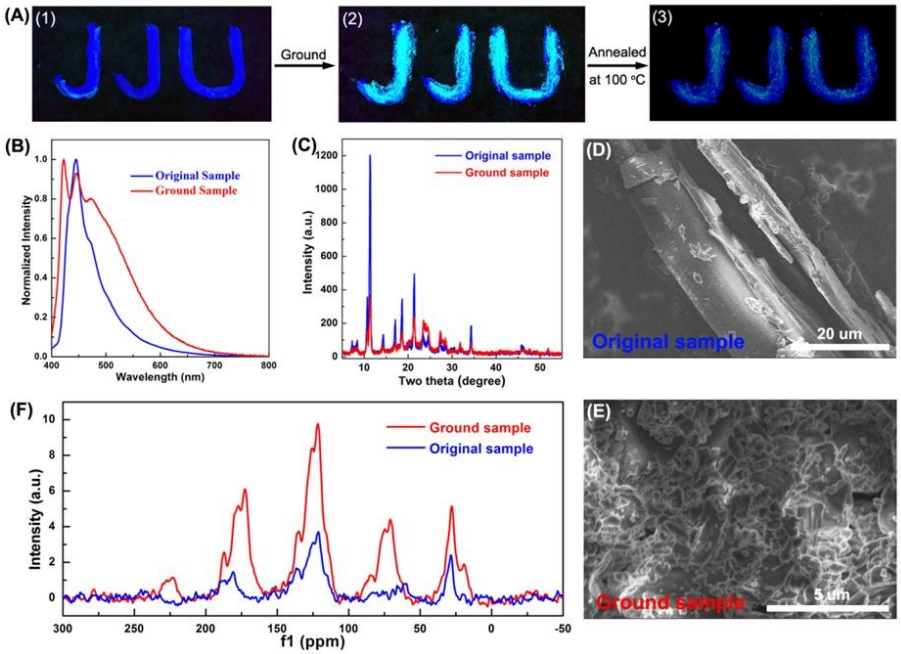

Figure 2. (**A**) Pictures of JJU with different treatment taken under UV irradiation (365 nm); (**B**) Fluorescence spectra of **5** in different solid states, excitation wavelength: 370 nm; (**C**) XRD profiles of original powder and powder after grinding; (**D-E**) SEM images of **5** in different solid states (D: original sample, E: ground sample); (**F**) Solid-state ^{13}C NMR spectra of **5** (blue: original sample, red: ground sample).

(Figure S4), indicating the weak charge transfer interactions in this system, which is highly consistent with experimental results. In addition, the spectral behaviors for compound **5** in solution and solid states as well as thin film were also measured (Figure S5). The thin films were deposited onto a glass substrate via spin coating. A significant red-shift (45 nm) for compound **5** can be observed in the emission of solid powder compared with solution. What is more, the thin film of **5** generated significant multi-emissions ranging from 423 to 534 nm. The interesting emission features will impart **5** great potential in further manipulation of multiple energy levels of solid-state organic luminophor toward a greatly widened scope of applications. Meanwhile, the absorption of compound **5** solved in CH_2Cl_2 and thin film were also explored. As shown in Figure S5, the barely changed UV-vis spectra between solution and thin film will undoubtedly hint at the existence of excimers. [67-68]

To gain a deeper insight into the electrochemical property, the cyclic voltammetry (CV) of **5** was performed in dichloromethane (Figure S6-S7). All measurements were carried out at room temperature with a conventional three-electrode (the working electrode: glassy carbon electrode, the reference electrode: saturated calomel electrode (SCE), and a platinum wire as the auxiliary electrode). Ferrocene/ferrocenium redox couple (Fc/Fc^+) was used as an internal reference. The oxidation and reduction waves of **5** were irreversible, indicating the instability of the produced radical ion. Actually, the CV measurements in combination with the relevant empirical formulas can also be used to calculate the HOMO and LUMO levels.[69-70] The HOMO and LUMO levels were estimated to be -5.61 eV, -1.98 eV, respectively, which were in good agreement with the calculated values (-5.71, -2.01 eV, Figure S8).

As expected, molecule **5** displayed satisfactory MCL properties with merits of high contrast and fast response as shown in Video S1 and Figure 2A. The as-prepared sample exhibited a light blue emission under a 365 nm UV light, afterwards changed directly to cyan upon mechanical grinding. It proves that the proper boron-nitrogen molecules indeed possess excellent MCL features, confirming our original design strategy.

Since the designed MCL material shows high contrast and sensitivity luminescence behavior, its applied potential in optical recording was further explored as well. Letters "JJU" were written on weighing paper with **5** as ink dissolved in CH_2Cl_2 (Figure 2A-1).When grinding up on, the high contrast cyan letters appear directly (Figure 2A-2). The high contrast cyan letters appear instantly when applied in grinding (Figure 2A-2), yet nearly faded with heating at 100°C for 1 min (Figure 2A-3), suggesting its accelerated self-reversible process under suitable temperature. These simple operations and color changes imply its quite prosperous applications for security ink, optical recording etc.

To further explore the mechanism of the color change under mechanical stimulation, solid-state photoluminescence spectra for both pristine and ground samples were measured. As shown in Figure 2B, the emission of original sample was centered at 445 nm, while after grinding two new shoulder peaks appeared at 422 nm, 472 nm, respectively. As known, the multiple emissions can effectively regulate the luminescence performance,[71-72] which are in good agreement with the observed MCL color change phenomenon. To confirm the relationship between mechanical force and luminescence, the quantitative experiments were conducted. As shown in Figure S9, with the increase of vertical pressure, the intensity of the emission peak at 470 nm increases

gradually. The results demonstrate that the magnitude of forces do have a significant effect on the luminescence behavior.

X-ray diffraction (XRD) and scanning electron microscopy (SEM) were performed to gain insight into the intrinsic mechanism of MCL (Figure 2C, Figure 2D-2E). The original sample **5** showed a sharp and intense diffraction peak at 2θ=11.4° followed by multiple peaks from 2θ = 14.3°-34.3°, namely a well-ordered microcrystalline structure. As noted, the as-prepared sample possesses typical crystalline state. While in *situ* grinding, conversely, some of the sharp peaks became evidently weak, suggesting that the major crystalline structure was destroyed through the mechanical force and presents a tendency to a quasi-amorphous state transition. The weakening or disappearance of the partial diffractions illustrate that the layered long-range order has been destroyed, while the significantly increasing diffractions (2θ =24.2°, 27.1°) suggest that the order within the monolayer has partially enhanced during the grinding process. According to Bragg equation, the distances (d) were 3.71 Å and 3.30 Å. Such a change in the diffraction angles implies an increase in the intermolecular π-π interaction distance,[73] which has a rational relation with the fluorescence intensity and significant impact on the fluorescence emission, further leading to the emission maximum changes. The above phenomena demonstrated that the interactions between layers in the pristine material **5** is tunable, and thus the position and packing modes between adjacent monolayers can be easily alternated upon grinding treatment. Furthermore, the SEM results, as shown in Figure 2D-2E also support this inference. The crystalline to quasi-amorphous transformation for solid-state **5** is consistent with the sample morphological changes before and after grinding, in which the long-range loose sheet-like morphology has splintered into tiny fragments upon force stimulus. Therefore, it is believed that grinding-induced MCL behavior of **5** can be attributed to the changes of stacking patterns and intermolecular interactions. To confirm it, the solid-state nuclear magnetic technology (NMR), which mainly focuses on the different local environments around various nuclei and can deliver rich and detailed information to distinguish subtle structure and around environment differences,[74] was employed as an assistant method.The chemical shift of ^{13}C-NMR was hence determined as the selected key signal regarding the possible changes of chemical environment in various states. As observed in Figure 2F, obvious change in the carbon nuclei appears after grinding, the type of carbon signal increases sharply with the phenomenon of signal enhancement, It hints that the molecules within a certain direction were in a much more constrained environment after grinding due to the partial enhanced intermolecular interactions, which was consistent with the results of the redshift emission and XRD. Solid-state nuclear magnetic technology has been recognized as a powerful and advantageous analytical tool for supporting exploration in the complex molecular interactions and molecular configurations. However, the potential of this method in discussing the MCL behaviors of luminescent materials have rarely been covered. In this regard, we firmly believe that solid-state NMR technology will contribute greatly in clarifying the mechanism of MCL with new directions of thinking, eventually promoting the development of organic smart materials.

To further evaluate the luminescence mechanism, the MCL behaviors of the corresponding hydrocarbon analogue **5′** was parallelly investigated.[75] Interestingly, no force-response for **5′** was observed at the same condition. Thus, we may conclude that the boron nitrogen unit assumes an irreplaceable role in regulating luminescence behavior in this system.

.

This raises an interesting issue, namely the two molecules of **5** and **5′**, despite very similar structure, present notably different MCL behaviors. The molecular packing and intermolecular interactions play an important role in bridging the natural properties of single molecules and the macroscopic optoelectronic performance of organic materials[23]. Therefore, to get insight into the different behaviors for **5** and **5′** under mechanical stimulation, the corresponding crystal structures were investigated in detail. We systematically analyzed the molecular stacking patterns and intermolecular interactions of the two emitters.

The single crystals of **5** suitable for X-ray analysis were obtained by recrystallization from solutions of dichloromethane and hexane. As shown in Figure S10, the five fused six-membered rings in **5** revealed a highly planar conformation. The B-N bond length in this structure is 1.402(3) Å, very close to the length of a localized B-N bond (1.403(2) Å),[76-77] which means that the π-electrons localized in B-N bond was consistent with those reported in BN aromatic systems, and shows distinct double-bond character. In addition, the B-C and N-C bond lengths (B-C8=1.527(3), N-C6=1.403(2) Å) in **5** are noticeably shorter than normal B-C (ca. 1.579(5) Å) and N-C (ca. 1.47 Å) single bonds,[78] aligned with the electron delocalization over these atoms. The single crystal analyses reveal that molecule **5** is constructed based on a monoclinic crystal system, crystallizing in the space group C12/c1 (Cc-form) with eight molecules in one cell unit. These eight molecules present a unique spatial arrangement, forming two groups of antiparallel intersecting stacking modes. Meanwhile, the centroid positions of the two groups of molecules are completely overlapped (Figure 3A), benefitting from the high degree of symmetry, these molecules show special stacking patterns in three dimensions. For instance, in the direction of the b axis, the unique spatial arrangement favored to construct an ordered packing mode (Figure 3B), shaping multi-group remarkable offset π-π stacking, in which the average distance between layers is 3.669 Å. Along the π–π stacking direction, the crystals of **5** exhibit a straight line-packing pattern driven by the multiple intermolecular interactions(Figure S11 in the SI), including π···π, N-H···π and C-H···π interactions, with distances in the range of 3.61-4.0 Å (Figure S12 in the SI). It is worth mentioning that those interactions play a vital role in the single crystal cultivation. No accumulation pattern of **5** can be obtained as straight line without those interactions. More importantly, viewing from the c axis, the antiparallel intersecting stacking modes lead to forming multiple intersecting parallelograms (Figure 3C). As well known, parallelograms are inherently unstable and easily deform under the action of external forces, which therefore provides an opportunity to readjust the intermolecular interactions and stacking patterns, and endows **5** with excellent stimulus-responsive property.

In terms of crystal structure for **5′**,[79] the molecule exhibited asymmetric system with the space group of $P2_1$, and each cell contained four independent molecules with markedly different orientations, the dihedral angle between the least-squares planes through each of the molecules was 47.8 (8)°. The crystal packing adopted a γ-type structure, where molecules stacked in the direction of the b axis. The molecules within each stack formed offset face-to-face attractive contacts with a perpendicular distance of 3.740 Å, larger than the molecule **5**. Afterwards, we thoroughly examined the molecular packing mode in the crystals of **5′**. Interestingly, another set of molecules were inserted between the layers on the b axis.

View Article Online
DOI: 10.1039/D0TA06191C

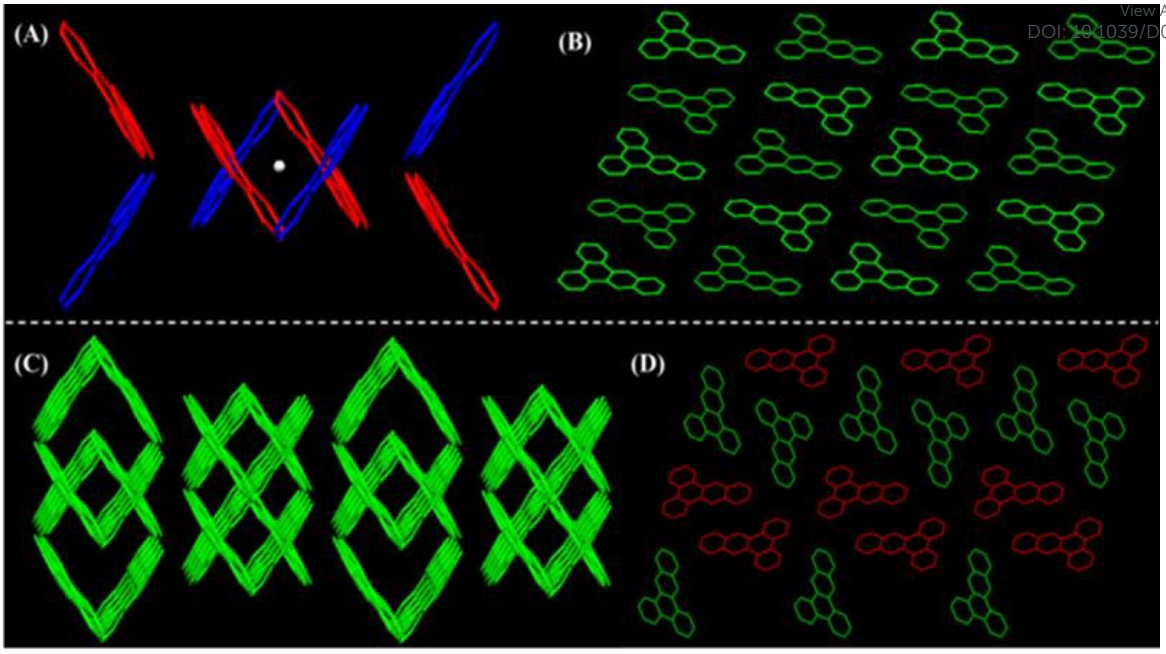

Figure 3. (**A**) Molecular conformation of **5** in one cell unit; (**B**) The molecular conformations of **5**; (**C**) The stacking patterns of **5** along the c axis; (**D**) The molecular conformations of **5′**.

These multiple molecular conformations yield an irregular packing mode, resulting in the absence of MCL effect. Single crystal analysis demonstrated that the molecular packing and intermolecular interactions play significant roles in the MCL light-emitting process, and the MCL properties are likely to perish after subtle modifications of the molecular structure. Therefore, to expound the direct relation of MCL property and the suitable molecular packing modes, phenylamine moiety was introduced to eliminate the molecular packing effect, the crystal analysis showed no remarkable π-π interactions for the referential compound **6** (Figure S14 in the SI**)**. As expected, no MCL emission was observed for referential compound **6** upon grinding. This comparative experiment further revealed the significant effect of molecular packing on MCL properties from an alternative perspective.

Another intriguing question is why did the very similar structured **5** and **5′** show completely different stacking patterns. Molecular electrostatic potential surface maps (ESP) and the dipole moment have been used to visualize and understand the molecular packing modes.[80-83] Consequently, to explore reasons behind the changes of **5** and **5′** molecular packing, we calculated the ESP maps and the dipole moments of the two molecules, respectively. For molecular **5′**, no significant separation between positive and negative potentials was observed. However, upon substitution of C=C fragmentwith isoelectronic B-N unit, the ESP around the nitrogen atom in **5** turned positive (Figure 4), indicating that it is an electron acceptor. Interestingly, we cannot find any negative potential on the potential surface, conversely, dispersing throughout the whole conjugate skeleton, which can effectively disperse and diminish the electron density, leading to a weaker intermolecular electrostatic repulsion and thus smaller π-π stacking distances. Moreover, the electrostatic potential presented a positive edge and negative center distribution mode, which is conducive to forming offset face-to-face packing mode rather than the face-to-face stacked geometry.[84] This is highly consistent with the crystals data. Furthermore, the dipole moment was introduced to discuss the packing patterns. As shown in Figure S15, the dipole moment of **5** (1.3541 Debye) is much larger than that of **5′** (0.0094 Debye), and the dipole vector extends in accordance to the direction of the B-N bond, through the C-B-N angle. Benefitting from the increase of the dipole moment, the monolayer preferred the offset-stacked geometries in accordance with the dipole moment vector's position and direction. Such offset face to face packing mode can significantly strengthen the electrostatic attraction and avoid the electrostatic repulsion. Meanwhile, the adjacent groups of molecules tend to form antiparallel packing mode, and such antiparallel packing pattern indeed contribute greatly to less the Coulomb repulsion. Thus, as mentioned above, the parallel tetrahedral column stacks are formed along c axes. The results demonstrated that introducing the boron nitrogen unit strategy is valid to regulate molecular packing modes and intermolecular interactions and thus endow certain boron nitrogen aromatic materials with the MCL property.

As previously mentioned, the exploration of light-emitting process is highly desirable to reveal the mechanism of force-stimuli response. In traditional photoluminescence (PL) and electroluminescence (EL) processes, inherent energies like the excited singlet (S) and highly sensitive triplet (T) states also exist in the MCL process[17,30]. Therefore, the strength of intersystem crossing (ISC) may also have a great influence on MCL phenomena. Thus, time-dependent density functional theory (TD-DFT) calculations were respectively performed on the isolated molecule and dimers (selected from the single-crystal structure) to identify the actual status of the energy level in the singlet and triplet states.The energy level diagrams and excited state transition configurations for singlet and triplet states are presented in Figure 4, Figure S16 and Table S5-S8. The red orbitals refer to the effective ISC channels. Typically,

View Article Online
DOI: 10.1039/D0TA06191C

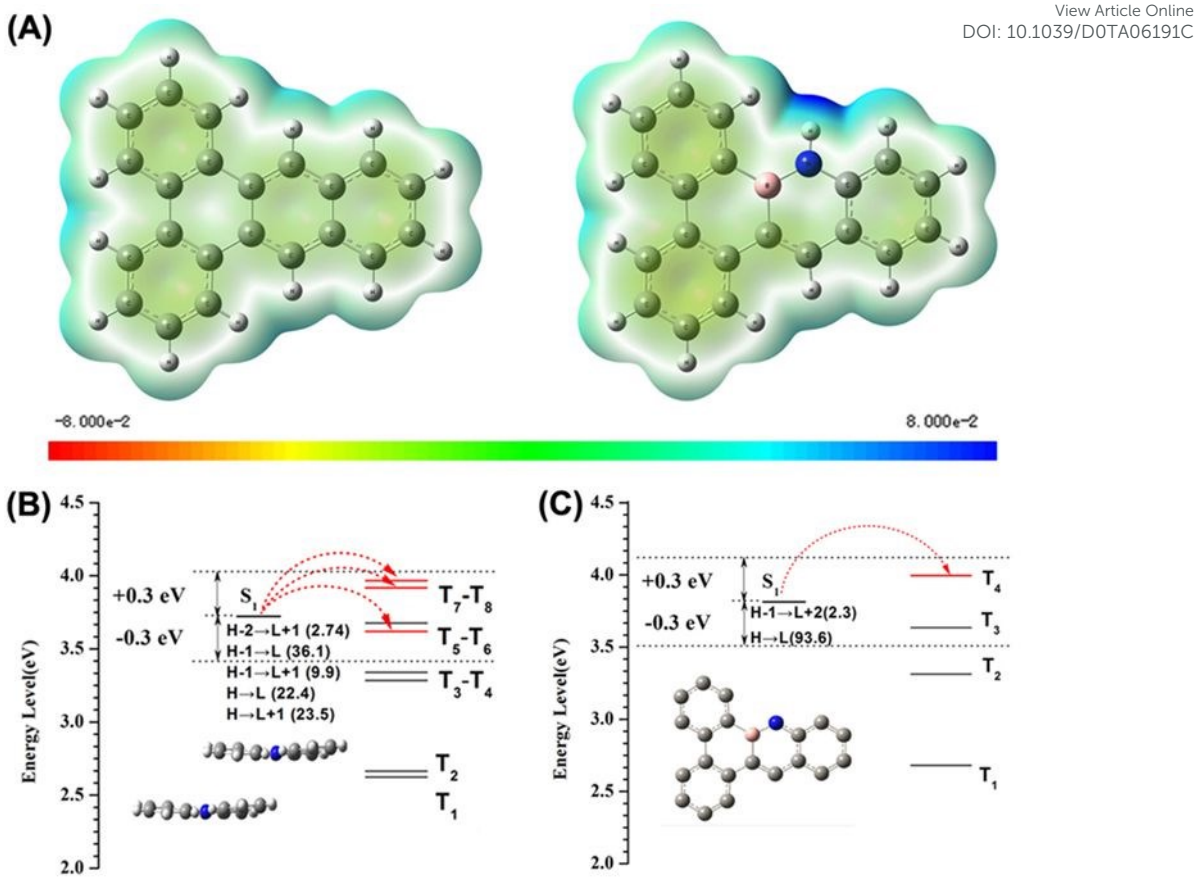

Figure 4. (**A**) ESP maps of **5** and **5′** (left: **5′**, right: **5**); (**B-C**) Energy level diagrams and possible ISC channels from excited singlet state (S_1) to excited triplet states (T_n) for **5** (B: Dimer; C: Isolated)

when triplet (Tn) states contain the same transition orbital compositions as excited S1 as well as an energy gap within ± 0.3 eV, the singlet-to-triplet transition from S_1 to T_n is considered as the valid channel for the intersystem crossing. [17, 85-86] Concerning the hydrocarbon analogue **5′** dimers, there were three minor ISC channels from S_1 to T_7, T_8, T_9 with the energy gaps of -0.1228, -0.1497 eV, -0.2600 eV, respectively. As for the **5** dimers, the main channel is completely opened, and one main and two minor channels were formed as well from S_1 to T_n (T_5, T_7, T_8) with the energy gaps ranging from 0.0904 to -0.2319 eV. All of the matched Tn states share certain parts of the same transition orbital compositions with the S_1 state (H→L, H→L+1, H-1→L, H-1 → L+1, H-2 → L+1). The ISC, known as a nonradiative relaxation process from excit singlet state to excited triplet state, is usually detrimental to the fluorescence emission. However, upon grinding, the effective ISC channels were destroyed. Indeed, only one minor ISC channel for the isolated **5** molecule existed, and thereby the non-radiation transition with the energy loss decreases dramatically, leading to the enhanced radiative transition contributed to the fluorescence behavior, and thus resulting in the bright emission in the radiation process. In sharp contrast, for counterpart **5′**, compared the dimer and monomer, only one minor ISC channel was destroyed, meaning that the transition forms are almost unchanged before and after grinding. Therefore, from the perspective of calculation, it is also demonstrated that compound 5¢ does not possess the phenomenon of MCL.

Herein, we proposed a possible mechanism to elucidate MCL emission process using a hybrid crystal analysis and theoretical calculations method. The embedded boron nitrogen unit could significantly modify the electronic distribution and polarity of the molecule **5**, and create unique intermolecular interactions, which lead to form the special stacking patterns and the enhanced ISC transition. Apparently, nonradiative ISC channel and radiative transition are conflict in terms of fluorescence emission. In the original aggregation states, the enhanced ISC transition effectively opens the nonradiative channels to the highly sensitive and nonemissive triplet states, resulting in the weak fluorescence state. Conversely, upon mechanical stimulus, the solid-state morphology and the radiation patterns were manipulated. The non-radiation channels were destroyed accordingly, afterwards enabling the radiative transition dominates light-emitting process to yield the bright fluorescence state. Thus, a conclusion can be drawn that the formation and fracture of ordered molecular aggregates with efficient intermolecular interactions is deemed to be the favorable factors for the MCL behavior in the light-emitting process.

Conclusions

In summary, we proposed a molecular-level design strategy to achieve a novel MCL material by incorporating BN unit into

highly planar and rigid aromatic backbone. The isoelectronic analogues of **5** and **5′** with distinctly different MCL activities in this work can help us to make a deep understanding of the structure-packing-performance relationship, guiding the design of organic molecules with MCL property. Basically, the easily adjustable packing modes with enhanced intermolecular interactions make it fundamentally conducive to achieve the MCL property. In this case, the introduction of boron nitrogen unit led to forming parallelogram molecule packing, which is easily deformed and recovered in comparison with other packings such as the triangle. This typical example provided a good template to explore the new strategies for optimizing the molecular packing in the future. Additionally, theoretical calculations confirmed the existence of some inherent energies like singlet (S) state and triplet (T) state in the MCL process, which provides an additional approach to understand the emission process. In short, the incorporation of boron nitrogen unit into polycyclic aromatic hydrocarbons is a promising strategy to develop intelligent luminescent materials, and the design strategy makes a big step in expanding the scope of the MCL family.

Conflicts of interest

There are no conflicts to declare.

Acknowledgements

This work was supported by the National Natural Science Foundation of China (Nos. 21861022, 21864015), Project funded by China Postdoctoral Science Foundation (No. 2019M662275), the key project of natural science foundation of Jiangxi Province (20202ACBL213003), and the Education Department of Jiangxi Province Foundation of China (Nos.GJJ190896, GJJ190927), National undergraduate innovation and entrepreneurship project (201911843012). The author would like to thank Wu Zhiyong from Shiyanjia Lab for the DFT calculation.

Notes and references

1. L. Liu, X. Wang, N. Wang, T. Peng, and S. Wang, *Angew. Chem. Int. Ed.*, 2017, **56**, 9160.
2. Y. Xie, and Z. Li, *Chem*. 2018, **4**, 943.
3. C.-X. Chen, Z.-W. Wei, Y.-N. Fan, P.-Y. Su, Y.-Y. Ai, Q.-F. Qiu, K. Wu, S.-Y.; Yin, M. Pan, and C.-Y. Su, *Chem.* 2018, **4**, 2658.
4. L. Gu, H. Shi, M. Gu, K. Ling, H. Ma, S. Cai, L. Song, C. Ma, H. Li, G. Xing, X. Hang, J. Li, Y. Gao, W. Yao, Z. Shuai, Z. An, X. Liu, and W. Huang, *Angew. Chem. Int. Ed.,* 2018, **57**, 8425.
5. Y. Zhan, H. Yang, H. Ma, G. Bian, Q. Zang, J. Sun, C. Zhang, Z. An, and W.-Y. Wong, *Angew. Chem. Int. Ed.,* 2019, **58**, 8773.
6. Q. Li, H. Zhu, and F. Huang, *J. Am. Chem. Soc*. 2019, **141**, 13290.
7. C. Wang, Y. Yuan, C. Ren, Q. Liao, J. Wang, Z. Chai, Q. Li, and Z. Li, *Matter,* 2020*,* **2***,* 181;
8. Y. Cheng, J. Wang, Z. Qiu, X. Zheng N. L. C.,Leung, J. W. Y. Lam, and B. Z. Tang, *Adv. Mater*. 2017, **29**, 1703900.
9. J. Picard, *Science*, 1939, **89**, 460.
10. N. C. Eddingsaas, and K. S. Suslick, *Nature*, **2006**, *444*, 163.
11. N. C. Eddingsaas, and K. S. Suslick, *J. Am. Chem. Soc*., **2007**, *129*, 6718.
12. J. Wang, J. Mei, R. Hu, J. Sun, A. Qin, and B. Z. Tang, *J. Am. Chem. Soc.* 2012, **134**, 9956.
13. B. Xu, W. Li, J. He, S. Wu, Q. Zhu, Z. Yang, Y. Wu, Y. Zhang, C. Jin, P. Lu, Z. Chi, S. Liu, J. Xu, and M. R. Bryce, *Chem*. *Sci*. 2016, **7**, 5307.
14. B. Xu, J. He, Y. Mu, Q. Zhu, S. Wu, Y. Wang, Y. Zhang, C. Jin, C. Lo, Z. Chi, A. Lien, S. Liu, and J. Xu, *Chem. Sci*. 2015, **6**, 3236.
15. Z. Ma, Z. Wang, X. Meng, Z. Ma, Z. Xu, Y. Ma, and X. Jia, *Angew. Chem. Int. Ed.* 2016, **55**, 519.
16. C. Wang, B. Xu, M. Li, Z. Chi, Y. Xie, Q. Li, and Z. Li, *Mater. Horiz*., 2016, **3**, 220.
17. J. Yang, X. Gao, Z. Xie, Y. Gong, M. Fang, Q. Peng, Z. Chi, and Z. Li, *Angew. Chem. Int. Ed*., 2017, **56**, 15299.
18. L. Huang, L. Liu, X. Li, H. Hu, M. Chen, Q. Yang, Z. Ma, and X. Jia, *Angew. Chem. Int. Ed.,* 2019, **58**, 16445.
19. G. Huang, Q. Xia, W. Huang, J. Tian, Z. He, B.-S. Li, and B. Z. Tang*, Angew. Chem. Int. Ed.,* 2019*,* **58***,* 17814.
20. S. Xu, T. Liu, Y. Mu, Y. Wang, Z. Chi, C. Lo, S. Liu, Y. Zhang, A. Lien, and J. Xu, *Angew. Chem.Int. Ed.,* 2015, **54**, 874.
21. Z. Chi, X. Zhang, B. Xu, X. Zhou, C. Ma, Y. Zhang, S. Liu, and J. Xu, *Chem. Soc. Rev.*, 2012, **41**, 3878.
22. Z. Yang, Z. Chi, Z. Mao, Y. Zhang, S. Liu, J. Zhao, M. P. Aldred, and Z. Chi, *Mater. Chem. Front.*, 2018, **2**, 861.
23. Q. Li, and Z. Li, *Acc. Chem. Res*. 2020, **53**, 962.
24. J. R. Xu,and Z. G. Chi, *Mechanochromic Fluorescent Materials: Phenomena, Materials and Applications*, The Royal Society of Chemistry: London, 2014.
25. Z. Ma, Z. Wang, M. Teng, Z. Xu, and X. Jia, *ChemPhysChem*. **2015**, *16*, 1811.
26. J. Chen, Q. Peng, X. Peng, L. Han, X. Wang, J. Wang, and H. Zeng, *ACS Appl. Polym. Mater.* 2020, **2***,* 1092.
27. S. Yagai, S. Okamura, Y. Nakano, M. Yamauchi, K. Kishikawa, T. Karatsu, A. Kitamura, A. Ueno, D. Kuzuhara, H. Yamada, T. Seki, and H. Ito, *Nat. Commun*. 2014, **5**, 4013.
28. C. Wang, and Z. Li, *Mater. Chem. Front*. 2017, **1**, 2174.
29. Y. Xie, J. Tu, T. Zhang, J. Wang, Z. Xie, Z. Chi, Q. Peng, and Z. Li, *Chem.Commun*. 2017, **53**, 11330.
30. J. Yang, Z. Ren, Z. Xie, Y. Liu, C. Wang, Y. Xie, Q. Peng, B. Xu, W. Tian, F. Zhang, Z. Chi Q. Li, and Z. Li, *Angew. Chem., Int. Ed.,* 2017, **56**, 880.
31. K. Nagura, S. Saito, H. Yusa, H. Yamawaki, H. Fujihisa, H. Sato, Y. Shimoikeda, and S. Yamaguchi, *J. Am. Chem. Soc.* 2013, **135**, 10322.
32. Y. J. Dong, B. Xu, J. B. Zhang, X. Tan, L. J. Wang, J. L. Chen, H.G. Lv, S. P. Wen, B. Li, L. Ye, B. Zou, and W. J. Tian, *Angew. Chem. Int. Ed.,* 2012, **51**, 10782.
33. Y. Wang, X. Tan, Y. M. Zhang, S. Y. Zhu, I. Zhang, B. H. Yu, K. Wang, B. Yang, M. J. Li, B. Zou, and S. X. A. Zhang, *J. Am. Chem. Soc.* 2015, **137**, 931.
34. W. Zhao, Z. He, Q. Peng, J. W. Y. Lam, H. Ma, Z. Qiu, Y. Chen, Z. Zhao, Z. Shuai, Y. Dong, and B. Z. Tang, *Nat. Commun*. 2018, **9**, 3044.
35. Y. Q. Dong, J. W. Y. Lam, and B. Z. Tang, *J. Phys. Chem. Lett.* 2015, **6**, 13429.
36. J. Wang, Z. Chai, J. Wang, C. Wang, M. Han, Q. Liao, A. Huang, P. Lin, C. Li, Q. Li, and Z. Li, *Angew. Chem. Int. Ed*., 2019, **58**, 17297.
37. F. Liu, Z. Tu, Y. Fan, Q. Li, and Z. Li, *ACS Omega*. 2019, **4**, 18609.
38. X. Wang, X. Yao, A. Narita, and K. Müllen, *Acc. Chem. Res*. 2019, **52**, 2491.
39. W. Jiang, Y. Li, and Z. Wang, *Chem. Soc. Rev*. 2013, 42, 6113.
40. F. Jäkle, *Chem. Rev*. 2010, **110,** 3985.
41. T. Baumgartner, and R. Réau, *Chem. Rev*. 2006, **106**, 4681.
42. M. Stępień, E. Gońka, M. Żyła, and N. Sprutta, *Chem. Rev*. 2017, **117**, 3479.
43. W. Jiang, Y. Li, and Z. Wang, *Chem. Soc. Rev*. 2013, **42**, 6113.

44. Y. F. Geng, A. L. Tang, K. Tajima, Q. D. Zeng, and E. J. Zhou, *J. Mater. Chem. A*, 2019, **7**, 64.
45. Z. X. Cai, M. A. Awais, N. Zhang, and L. P. Yu, *Chem*, 2018, **4**, 2538.
46. Q. Miao, *Adv. Mater.* **2014**, *26*, 5541.
47. M. M. Morgan, and W. E. Piers, *Dalton Trans*. 2016, **45**, 5920.
48. M. J. D. Bosdet, and W. E. Piers, *Can. J. Chem*., 2009, **87**, 8.
49. C. R. McConnell, and S.-Y. Liu, *Chem. Soc. Rev*. 2019, **48**, 3436.
50. Z. X. Giustra, and S.-Y. Liu, *J. Am. Chem. Soc*. 2018, **140**, 1184.
51. P. G. Campbell, A. J. V. Marwitz, and S.-Y. Liu, *Angew. Chem. Int. Ed*., 2012, **51**, 6074.
52. X. Y. Wang, J. Y. Wang, and J. Pei, *Chem. Euro. J.* 2015, **21**, 3528.
53. J.-Y. Wang, and J. Pei, *CCL*. 2016, **27**, 1139.
54. T. Hatakeyama, S. Hashimoto, S. Seki, and M. Nakamura, *J. Am. Chem. Soc.* 2011, **133**, 18614.
55. X. Y. Wang, H. R. Lin, T. Lei, D. C. Yang, F. D. Zhuang, J. Y. Wang, S. C. Yuan, and J. Pei, *Angew. Chem. Int. Ed*., 2013, **52**, 3117.
56. X. Y. Wang, F. D. Zhuang, X. Zhou, D. C. Yang, J. Y. Wang, and J. Pei, *J. Mater. Chem. C*. 2014, **2**, 8152.
57. X. Y. Wang, F. D. Zhuang, R. B. Wang, X. C. Wang, X. Y. Cao, J. Y. Wang, and J. Pei, *J. Am. Chem. Soc*. 2014, **136**, 3764.
58. F.-D. Zhuang, Z.-H. Sun, Z.-F. Yao, Q.-R. Chen, Z. Huang, J.-H. Yang, J.-Y. Wang, and J. Pei, *Angew. Chem. Int. Ed*., 2019, **58**, 10708.
59. E. Yamaguchi, C. Wang, A. Fukazawa, M. Taki, Y. Sato, T. Sasaki, M. Ueda, N. Sasaki, T. Higashiyama, and S. Yamaguchi, *Angew. Chem. Int. Ed*., 2015, **54**, 4539.
60. Y. J. Chen, W. N. Chen, Y. J. Qiao, X. F. Lu, and G. Zhou, *Angew. Chem. Int. Ed.,* 2020, **59**, 7122.
61. X.-Y. Wang, A Narita, X. Feng, and K. Müllen, *J. Am. Chem. Soc*. 2015, **137**, 7668.
62. H.; Huang, Y. Zhou, M. Wang, J. Zhang, X. Ca, S. Wang, D. Cao, and C. Cui, *Angew. Chem. Int. Ed*., 2019, **58**, 10132.
63. Z.-H. Zhao, L. Wang, S. Li, W.-D. Zhang, G. He, D. Wang, S.-M. Hou, and L.-J. Wan, *J. Am. Chem. Soc.* 2020, **142**, 8068.
64. S. R. Wisniewski, C. L. Guenther, O. A. Argintaru, and G. A. Molander, *J. Org. Chem*. **2014**, *79*, 365.
65. P. Chen, A. S. Marshall, S.-H. Chi, X. Yin, J. W. Perry, and F. Jäkle, *Chem. Eur. J.* 2015, **21**, 18237.
66. L. Ji, S. Griesbeck, and T. B. Marder, *Chem. Sci.* 2017, **8**, 846.
67.J. Vollbrecht, H. Bock, C. Wiebeler, S. Schumacher, H. Kitzerow, *Chem. Eur. J.* 2014, **20**, 12026.
68. J. Vollbrecht, C. Wiebeler, A. Neuba, H. Bock, S. Schumacher, H. Kitzerow, *J. Phys. Chem. C*, 2016, **120**, 7839.
69. J. Tauc, *Mat. Res. Bull.* 1968*,* **3**, 37.
70. C. -P. Chen, S. -H. Chan, T. -C. Chao, C. Ting and B. -T. Ko, *J. Am. Chem. Soc.*, 2008, **130**, 12828**.**
71. D. Tian, F. Qi, H. Ma, X. Wang, Y. Pan, R. Chen, Z. Shen, Z. Liu, L, Huang, W. Huang, *Nat. Commun.* 2018*,* **9**, 2688*.*
72. D. S. Karpovich, G. J. Blanchard, *J. Phys. Chem.* 1995*,* **99***,* 3951*.*
73. W. Li, Q. Huang, Z. Mao, J. Zhao, H. Wu, J. Chen, Z. Yang, Y. Li, Z. Yang, Y. Zhang, Matthew P. Aldred, and Z. Chi, *Angew. Chem. Int. Ed*., 2020, **59**, 3739.
74. M. Skotnicki, D. C. Apperley, J. A. Aguilar, B. Milanowski, M. Pyda, and P. Hodgkinson, *Mol. Pharmaceutics*, 2016, **13**, 211.
75. The commercially available compound **5′** was purchased from Sigma-Aldrich.
76. C. Ma, J. Zhang, J. Li, and C. Cui, *Chem. Commun.,* 2015, **51**, 5732.
77. D. Tian, J. Jiang, H. Hu, J. Zhang, and C. Cui. *J. Am. Chem. Soc.* 2012, **134**, 14666.
78. A. J. Ashe III, *Organometallic*s, 2009, **28**, 4236.
79. Note: **5′** as a reported compound, please refer to the following literature for relevant crystal data. P. Fernandes, A. Florence, K. Shankland, W. I. F. David, *Acta Cryst*. *2005*. **E61**, o1483.
80. C. J. Pace, and J. Gao, *Acc. Chem. Res.* 2013, **46**, 907.
81. S. E. Wheeler, *J. Am. Chem. Soc.* 2011, **133**, 10262.
82. L. M. Salonen, M. Ellermann, and F. Diederich, *Angew. Chem. Int. Ed*., 2011, **50**, 4808.
83. J.-H. Dou, Y.-Q. Zheng, Z.-F. Yao, Z.-A. Yu, T. Lei, X. Shen, X.-Y. Luo, J. Sun, S.-D. Zhang, Y.-F. Ding, G. Han, Y. Yi, J.-Y. Wang, and J. Pei, *J. Am. Chem. Soc.* 2015, **137**, 15947.
84. Christopher J. Pace, and J. Ga*o, Acc. Chem. Res.* 2013, **46**, 907.
85. G. Zhang, J. Chen, S. J. Payne, S. E. Kooi, J. N. Demas, and C. L. Fraser, *J. Am. Chem. Soc.* 2007, **129**, 8942.
86. S. Menning, M. Krämer, B. A. Coombs, F. Rominger, A. Beeby, A. Dreuw, and U. H. F. Bunz, *J. Am. Chem. Soc.* 2013, **135**, 2160.

Graphical abstract:

View Article Online
DOI: 10.1039/D0TA06191C

This paper reports on a novel molecular-level design strategy to achieve a novel MCL material by incorporating BN unit into highly planar and rigid aromatic backbone. We found that the introduction of boron nitrogen unit is the key to design the MCL smart materials, because it can tailor the molecular dipole moment and intermolecular interactions and therefore yield the MCL performance.